Rationalizing the design of hyaluronic acid-decorated liposomes for targeting epidermal layers: a combination of molecular dynamics and experimental evidence

Silvia Franzé[1], Francesco Rama[1], Paolo Rocco[1], Michela Debernardi[2], Valeria Bincoletto[2], Silvia Arpicco[2*], Francesco Cilurzo[1*]

[1]Department of Pharmaceutical Sciences – Università degli Studi di Milano-via G. Colombo 71, 20133, Milan, Italy

[2]Department of Drug Science and Technology - Università degli Studi di Torino-Via Giuria 9, 10124 Turin, Italy

*Authors to whom correspondence should be addressed:
francesco.cilurzo@unimi.it
silvia.arpicco@unito.it

Keywords: ***hyaluronic acid, liposomes, skin penetration, lipids, molecular design, skin pathologies***

Abstract

This work provides information on the features of low molecular weight hyaluronic acid (HA)-decorated liposomes to target resveratrol (RSV) in the skin. Deformable liposomes were made of soy-phosphatidylcholine with Tween 80 as the fluidizing agent. For HA conjugation, three different phosphoethanolamines were tested: 1,2-dipalmitoyl-*sn*-glycero-3-phosphoethanolamine (DPPE), 1,2-dimyristoyl-*sn*-glycero-3-phosphoethanolamine (DMPE) and 1,2-dioleoyl-*sn*-glycero-3-phosphoethanolamine (DOPE). The different phosphoethanolamine-HA conjugates were inserted into the liposome bilayer by hydration (HA on both faces of the bilayer) or by the postinsertion method (HA only on the external face of the bilayer). The effect of these variables on deformability was experimentally assessed by an in-house method (*K* value, the lower the value, the higher the deformability) and molecular dynamics (MD) simulations. The results showed that the *K* values of HA-liposomes obtained by hydration were higher than the *K* values of HA-liposomes prepared by postinsertion, and both were at least 10-fold higher than the *K* values of the corresponding plain liposomes. The nature of the lipid anchor played a key role in deformability (DMPE>DOPE>DPPE) with high variability in the case of DOPE formulations. These data were justified by the trends found in silico for the bilayer bending modulus and the HA end-to-end distance. In addition to liposome flexibility, the HA extent seems to be the key factor governing the skin penetration of RSV. The higher the extent is, the larger the amount of the drug retained in the skin. Regarding skin permeation, a parabolic trend was recorded, and the optimal amount to favour skin permeation was an approximately 30 HA/phospholipid (µg/mmol) ratio. This study reports the first evidence that it is possible to control drug delivery in the skin by tuning the amount of HA on the vesicle surface.

Introduction

Chronic inflammatory skin pathologies, such as atopic dermatitis (AD) and psoriasis, are occurring at an increasing incidence in the worldwide population, with significant use of economic resources for patient assistance. These pathologies are characterized by altered stratum corneum composition (AD) and abnormal epidermal proliferation (psoriasis) with consequent barrier dysfunction and inflammation[1]. The treatment and management of inflammatory skin diseases has a target in the upper skin layers, where the amount of delivered drug should be maximized, limiting systemic absorption.

Nevertheless, skin is an excellent barrier due to the peculiar composition and architecture of its external layer, the stratum corneum, which opposes the penetration of most locally applied

substances. Nanotechnology and deformable liposomes, in particular, have been widely exploited to overcome the stratum corneum barrier, with the aim of gaining access to the epidermis and dermis layers[2]. Several studies show that these drug delivery systems act as carriers of low- and high-molecular-weight compounds, facilitating the transport of a drug across the skin, regardless of its physicochemical characteristics. This behaviour is ascribed to the particular composition of such liposomes, which have a fluid bilayer and contain one or more destabilizing agents (e.g., single chain surfactant, ethanol) that allow the liposomes to rearrange their structure, elongating into the stratum corneum channels.[3,4] However, there is very little evidence in the literature about the functionalization of these liposomes with specific targeting moieties to reach specific diseased skin areas.

Hyaluronic acid (HA) is the major component of the extracellular matrix and is very abundant in the skin. This polysaccharide is well known for its multiple beneficial properties in the field of both pharmaceutical and cosmetic products, including hydration and antiaging effects, and for its role in enhancing wound healing.[5] HA also has anti-inflammatory and antiangiogenic effects[6]. In addition to these properties, low molecular weight HA is able to permeate the skin, favouring the penetration of coadministered compounds.[7,8,9] Moreover, the major HA receptor, CD44, is involved in normal epidermal function, regulating the proliferation and differentiation of keratinocytes.[5] Overexpression of this receptor was found in tumour cells and in AD and psoriatic skin,[1,5] thus making HA-based carriers potential candidates for the treatment of several skin diseases characterized by alteration of the epidermis structure and functionality. HA may then be an attractive moiety for targeting diseased skin tissues.

In a previous study, we demonstrated the feasibility of exploiting HA-decorated deformable liposomes to favour the accumulation of the carried drug in the epidermis for the treatment of local pathologies. However, the decoration of the surface of liposomes with HA also affects the deformability properties of the bilayer to some extent, requiring an adjustment of the formulation[10]. This behaviour has been ascribed not only to the binding of HA to the lipid bilayer but also to the additional phospholipid used as an HA anchor (i.e., 1,2-dipalmitoyl-*sn*-glycero-3-phosphoethanolamine, DPPE). DPPE has been shown to be able to cause an important dose-dependent increase in bilayer stiffness, requiring the addition of ethanol as a further fluidizing agent to assure a suitable loading of HA without compromising the skin penetration ability of the prepared vesicles. In light of the promising effect of HA-decorated carriers to target the effect of topically applied drugs in the epidermis, this work aimed to better understand the role exerted by lipid composition, preparation method and HA dose on the properties of deformable liposomes, which will help to rationalize the design of liposomal formulations intended to be applied on the skin for the

treatment of skin inflammatory pathologies. To this end, low molecular weight HA (4800 Da) was chemically conjugated to three phosphoethanolamines (PEs) differing in chain length, degree of saturation and phase transition temperature (Tm), namely, the previously mentioned DPPE, 1,2-dimyristoyl-*sn*-glycero-3-phosphoethanolamine (DMPE) and 1,2-dioleoyl-*sn*-glycero-3-phosphoethanolamine (DOPE).

The conjugates were added to a bilayer composed of soy-phosphatidylcholine and Tween® 80 at different concentrations and using two different preparation methods, namely, hydration and postinsertion methods, to expose the HA moieties on both faces and on the outer face of the liposome membrane, respectively. The effect of these formulation variables on the deformability properties of liposomes was studied using a combination of experimental and in silico data to calculate the constant of deformability of the bilayer.

Molecular dynamics (MD) simulations were performed on three model membranes – representative of the liposomes studied experimentally – for which relevant properties, such as the area compressibility modulus and the bending modulus, were calculated. The results from MD simulations helped rationalize the effect of HA and the type of lipid anchor on the deformability of liposomes and were used to support the choice of formulation.

Finally, the effect of the selected variables on skin penetration ability was assessed in in vitro experiments carried out by using human skin as the membrane- and resveratrol (RSV)-loaded liposomes. RSV was selected as a model drug since it has a wide range of applications for topical use that move from antiaging action to positive effects in treating cutaneous autoimmune diseases such as atopic dermatitis and psoriasis[11]. Moreover, topical application of RSV is limited by both the poor skin permeation ability of this drug and its instability against light, heat and oxidation, which raises formulation concerns. The use of nanotechnology has already been proposed as a means to protect the drug from degradation while increasing the skin penetration ability.[12,13]

Experimental section

Materials

Soy-phosphatidylcholine (S100, s-PC) was kindly provided by Lipoid GmbH (Ludwigshafen, Germany). DPPE, DMPE and DOPE were obtained from Avanti Polar Lipids and Merck Italia (Rome, Italy), along with carbazole, ammonium molybdate and sodium dihydrogen phosphate. Hyaluronic acid 4800 Da was purchased from Lifecore Biomedical (Chaska, MN, USA). RSV was purchased from Labomar (Istrana, Italy). The DMPE-HA, DPPE-HA and DOPE-HA conjugates were

prepared following our previously described method for the preparation of the DPPE-HA conjugate.[14] Tween 80 was purchased from Croda (Chocques, France), whereas 4-(2-hydroxy- ethyl)piperazine-1-ethanesulforic acid (HEPES),ascorbic acid, HPLC grade and analytical-grade organic solvents were purchased from VWR (Milan, Italy).

Methods

Molecular Dynamics simulations.

In silico construction of the model bilayers.

A model bilayer consisting of 200 molecules (100 per leaflet) of L-alpha-phosphatidylcholine (Soy) (Soy PC, CAS no. 97281-47-5) was generated. One layer was constructed by clustering 100 molecules per leaflet with random rotations in VEGAZZ[15] and duplicating; two layers, each consisting of 12103 water molecules, were added (**System SoyPC**). The bilayer has been oriented so that the normal to the midplane of the bilayer is in the *z* direction.

In parallel, two conjugates were constructed in VEGAZZ from one molecule of either DMPE or DOPE and an HA oligomer of 12 repeating units (HA_{12}, MW ≈ 4500 Da) neutralized by the necessary number of Na ions, forming conjugates DMPE-HA and DOPE-HA, respectively. The HA oligomer was obtained by cleavage of the nonsulfonated HA_{20} chain utilized in a previous study.[16] Starting from System SoyPC, two random Soy PC molecules from each leaflet were replaced by two molecules of either DMPE-HA (**System DMPE**) or DOPE-HA (**System DOPE**). The necessary number of water molecules was removed to maintain the same number of heavy atoms as in System SoyPC (**Figure 1**). System DMPE and System DOPE, used as models to study the effect of the lipid anchor and of HA decoration, mimic, specifically, the bilayer of liposomes obtained by the hydration method (referenced below as L-DMPE-HA-H and L-DOPE-HA-H, respectively).

MD simulations were not performed on the system using DPPE as a lipid anchor. As we have already demonstrated in a previous study, the addition of DPPE alone leads to a significant increase of the bilayer's stiffness[10].

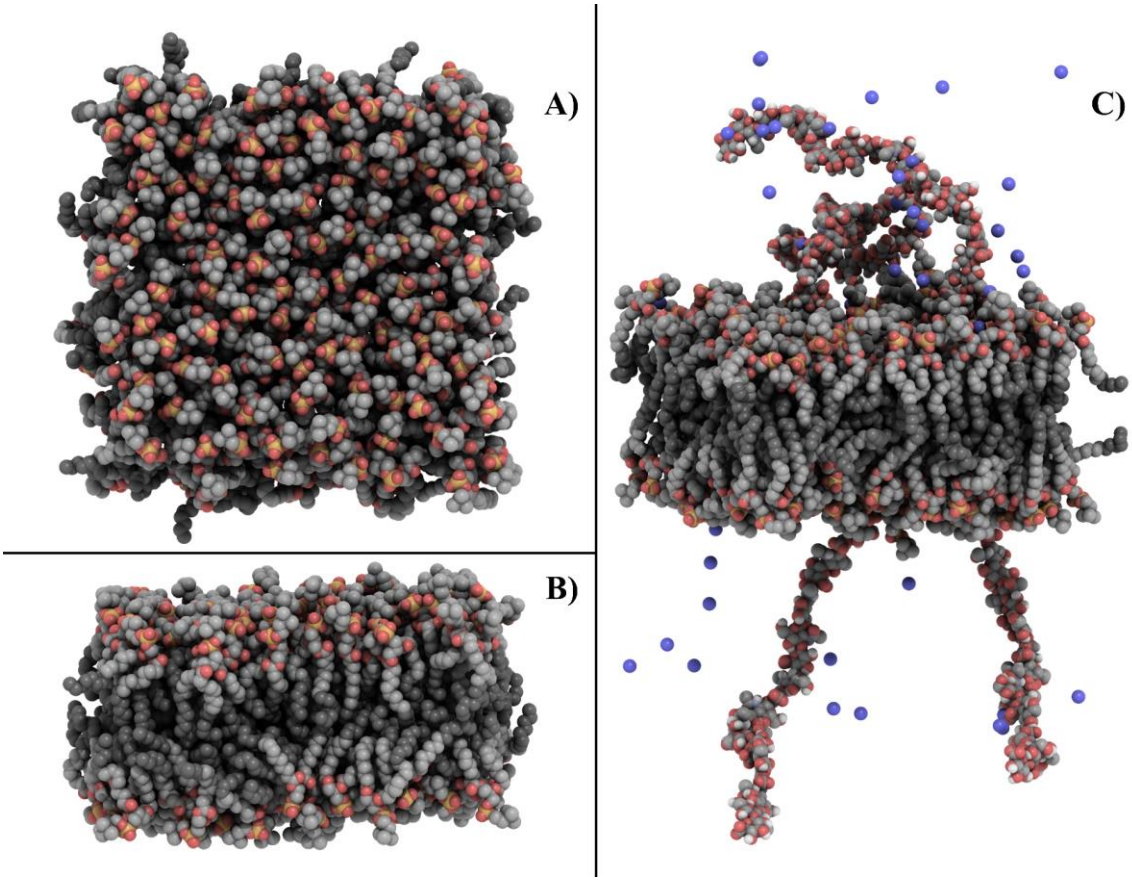

Figure 1. Model membrane (water molecules not shown) for System SoyPC (A, from top; B, from side) and System DOPE (C, from side, slightly rotated) at the end of equilibration run step 1. Blue dots represent Na^+ counterions. Image obtained with Qutemol.[17]

Each system was independently equilibrated through a 205-ns MD simulation at 300 K at a constant pressure of 1 atm (NPT) (equilibration run). The equilibration run was divided into two steps: a 150-ns simulation where a square cell was forced (x side = y sides) by disabling the use of a flexible cell option for faster convergence (equilibration step 1) and a 55-ns simulation where a flexible cell was allowed (equilibration step 2). Subsequently, each system underwent an 80-ns simulation (production run) used in the calculation of parameters at equilibrium. A minimization step and a heating step preceded equilibration step 1, equilibration step 2 and the 80-ns production run.

Molecular Dynamics simulation details.

Simulations were performed using NAMD[18] (nightly build 2020-11-01 Linux-x86_64-multicore-CUDA) on a PC assembled with off-the-shelf components, including an AMD Ryzen™ 9 processor and Nvidia® GeForce RTX graphic card, running Ubuntu 20.10 (kernel 5.8.0-26-generic GNU/Linux). The force fields used are CHARMM 36 for lipids and HA[19] and the TIP3P potential[20] for water. Data manipulation on simulation files was performed with scripts in the awk programming language[21] and Microsoft Excel.

All simulations were performed at 300 K at a constant pressure of 1 atm (NPT) with the following parameters: a) periodic boundary conditions were applied to stabilize the simulation space; b) Newton's equation was integrated using the r-RESPA method (every 4 fs for long-range electrostatic forces, 2 fs for short-range nonbonded forces, and 1 fs for bonded forces); c) the long-range electrostatic potential was computed by the particle mesh Ewald summation method, and the chosen cutoff length was 12 Å for both van der Waals and electrostatic potentials, with a switching function starting at 8 Å; d) the temperature was maintained at 300±10 K by Langevin's algorithm; e) Lennard-Jones (L-J) interactions were calculated with a cut-off of 10 Å, and the pair list was updated every 20 iterations; f) a frame was memorized every 10 ps in the 150 ns equilibration run and every 1 ps in the 55-ns run; and g) no constraints were imposed on the systems. Other simulation parameters are the same as described in a previous study.[22]

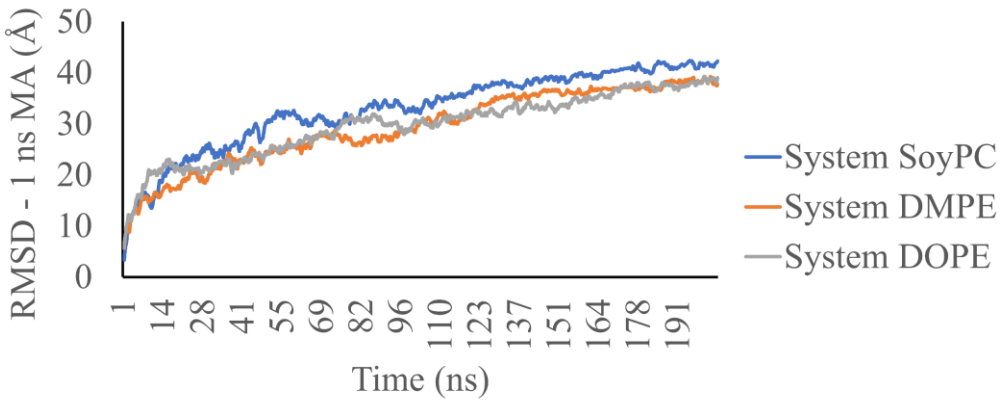

Figure 2. 1-ns moving average (MA) of a) RMSD (Å) for the equilibration run. Hydrogen atoms, DxPE-HA chains and water molecules were excluded from the calculation of RMSD.

Equilibration run

The root mean square deviation (RMSD, **Figure 2**) with respect to the first frame of the simulation ($t = t_0$), defined as $RMSD(t) = \sqrt{\sum_{i=1}^{N}(\vec{r}_i(t) - \vec{r}_i(t_0))^2/N}$ - where N is the number of atoms considered, $\vec{r}_i(t)$ is the position of atom i at time step t, and $\vec{r}_i(t_0)$ - shows that the system reached a stable conformation at the end of the 205-ns equilibration run. Water molecules, HA chains and hydrogen atoms were excluded from the calculation of RMSD.

Preparation of liposomes

Liposomes were prepared by the thin lipid film hydration method. In general, phospholipids (s-PC, DPPE or DMPE or DOPE), Tween 80 (T80) and, when required, RSV were dissolved in chloroform and mixed in suitable ratios in a round bottom flask (**Table 1**). The organic solvent was evaporated under reduced pressure for 1 hour by using a rotavapor (RII, Büchi, Italy) to allow the formation of

the lipid film. The film was then hydrated (for 1 hour at 40 °C) with the proper volume of 20 mM HEPES buffer (pH 7.4) to a final lipid concentration of 3% w/v. Liposomes resulting in the random orientation of HA on the external surface and into the aqueous core of liposomes were prepared by adding 3% mol/mol (with respect to s-PC) PE-HA conjugate in HEPES buffer during film hydration. To have HA only on the external leaflet of the liposomes, the "postinsertion method" was used. Empty liposomes were prepared as described above and mixed with DMPE/DOPE-HA conjugate dissolved in the minimum amount of HEPES buffer (to have a 1.5% mol/mol soy-PC-PE-HA ratio). The liposome/HA-conjugate mixture was then incubated at 30 °C for two hours and stirred at 300 rpm.

In all cases, liposomes were extruded (Avanti® Mini-Extruder, Avanti Polar Lipids, Inc.) 5 times through 0.2-μm and then 6 times through 0.1-μm polycarbonate membranes (Nuclepore® Track-Etch Membrane Polycarbonate – Nucleopore – UK) to obtain small unilamellar vesicles.

Finally, the formulations were purified from unencapsulated material by molecular exclusion chromatography on Sepharose CL-4B columns and eluted with HEPES buffer.

Table 1- Qualiquantitative composition (% w/w) of prepared liposomes

Formulation	Composition of lipid bilayer							
	s-PC	**T80**	**DMPE**	**DOPE**	**DPPE-HA**	**DMPE-HA**	**DOPE-HA**	**RSV**
L	85	15	-	-	-	-	-	-
L-DPPE-HA H	69.4	15	-	-	15.6	-	-	-
L-DPPE-HA PI	76.5	15	-	-	8.5	-	-	-
L-DMPE-HA H	69.4	15	-	-	-	15.6	-	-
L-DMPE-HA PI	76.5	15	-	-	-	8.5	-	-
L-DOPE-HA H	69.4	15	-	-	-	-	15.6	-
L-DOPE-HA PI	76.5	15	-	-	-	-	8.5	-
L-DMPE PI	83.9	15	1.1	-	-	-	-	-
L-DMPE H	82.9	15	2.1	-	-	-	-	-
L-DOPE PI	83.8	15	-	1.2	-	-	-	-
L-DOPE H	82.5	15	-	2.5	-	-	-	-
L RSV	85	15	-	-	-	-	-	2*
L-DMPE-HA H RSV	69.4	15	-	-	-	15.6	-	2*
L-DMPE-HA PI RSV	76.5	15	-	-	-	8.5	-	2*
L-DOPE-HA PI RSV	76.5	15	-	-	-	-	8.5	2*

Legend: *H: hydration method; PI: postinsertion method;* *the amount of active ingredient is expressed in mg/mL

Liposome physicochemical characterization

Particle size distribution and surface charge

The particle size distribution and ζ potential of the prepared liposomes were measured by dynamic light scattering (DLS) using a Zetasizer (Nano-ZS, Malvern Instrument, UK). Liposomal dispersions

were diluted 10 times with ultrapure water prior to being inserted into a disposable cuvette and analysed with a detection angle of 173°. ζ-Potential analyses were also performed on the diluted samples inserted in a capillary cell. Measurements were performed at 25 °C. Each measurement was replicated three times to obtain average data.

Phospholipid assay

The phospholipid concentration was measured according to a modified Rouser method[23], which basically quantifies the content of phosphate after cleavage of phospholipids with perchloric acid. Sodium dihydrogen phosphate at known concentrations was used as the standard.

For the assay, empty tubes (control), liposome samples and standard were heated in separate tubes to 100 °C until complete evaporation. Three hundred microlitres of perchloric acid (70%) was added to each tube and heated at 200 °C for 20 min. The samples were cooled, and 1 mL of purified water and 400 μL ammonium molybdate (1.25% w/v) were added to each tube and vortexed. Four hundred microlitres of ascorbic acid (5% w/v) was added, and after mixing, the tubes were heated at 100 °C for another 5 min. At this stage, samples containing phosphate turned blue. Finally, the absorbance of the samples and standard was read at 820 nm. The concentration of lipids was calculated based on the proportion of the sample and standard absorbances, with the standard concentration fixed at 40 nmol/μL.

Hyaluronic acid quantification

HA quantification was assessed by carbazole assay.[24] For the test, HEPES buffer was used as the "blank" sample, and liposome formulations with 0% HA were used as the "control" to assess the interference of the phospholipid in the colorimetric assay (the bilayer composition was the same as the bilayer composition of the sample under test). Liposomal dispersions were diluted to 1 mL with ultrapure water. Three millilitres of a 25 mM solution of sodium tetraboratedecahydrate in 96% sulfuric acid w/v was added to each tube, mixed and heated at 100 °C for 10 min in a water bath. The samples were then cooled under running water for 15 min prior to adding 100 μL of a 0.125% w/v carbazole solution in absolute ethanol. After mixing, tubes were heated again at 100 °C for 10 min. Finally, after cooling, the absorbance was read at 530 nm using a UV spectrophotometer (Lambda 25 UV/VIS spectrometer, PerkinElmer Life and Analytical Sciences, Singapore). Blank and control absorbances were subtracted from the absorbance of each sample, and then the concentration was estimated based on a calibration curve built using raw HA in the concentration range of 10–80 μg/mL. Three different samples for each formulation batch were assayed each time to obtain the mean HA content.

Quantification of RSV and determination of the encapsulation efficiency

For the determination of the amount of encapsulated RSV, after purification, liposomes were diluted in methanol (1:100 dilution). The RSV concentration was estimated by High Pressure Liquid. Chromatography (HLPC HP 1100 Chemstations, Agilent Technologies, Waldbronn, Germany) using a Waters Spherisorb ODS2 250 x 4.6 mm, 5 μm as the column. A mixture of methanol:Milli-Q® water:acetic acid (50:49.5:0.5 v/v) was used as the mobile phase; the flow rate was 1 mL/min, the thermostat was set at 30 °C and the UV/VIS lamp at 304 nm. Under these conditions, the retention time of RSV was 5.4 min. For the quantification of RSV, two different calibration curves in the concentration ranges 0.05 μg/mL– 5 μg/mL and 1 μg/mL – 100 μg/mL were built.

The encapsulation efficiency was calculated as mg RSV/μmol of lipids. The encapsulation efficiency percentage (EE %) was instead calculated according to the following equation:

$$\text{EE (\%)}=\frac{RSV(l)}{RSV\ (i)}X\ 100$$

where RSV (l) is the amount (mg/mL) of RSV found in the purified liposomal dispersion, and RSV (i) is the total amount of RSV (mg/mL) added to the lipid organic solution during the preparation of liposomes.

Deformability assay

The deformability of all liposomal formulations prepared was assessed by using a modified extrusion assay previously developed.[25] Prior to the test, all dispersions were diluted to the same lipid concentration (0.23 mM), and the number of vesicles was counted by nanoparticle trafficking analysis using a Nanosight300 (Malvern - UK) after a further 1:100 dilution of the samples with ultrapure water. Dispersions were then loaded into a gastight syringe that was inserted into an extruder casing fixed to a vertical holder, with the needle faced downward and the plunger end in contact with a 50-N loading cell of a mechanical dynamometer (INSTRON 5965, ITW Test and Measurement Italia S.r.l.; Italy). The steel probe was put in contact with the syringe plunger to force the liposome dispersion at a constant speed (1 mm/s) through a 50-nm polycarbonate membrane put in the extruder casing. To minimize the dead volume, before each test, the membrane was pretreated with 1 mL of ultrapure water. The force (N) required to displace the plunger was measured and plotted as a function of plunger displacement (mm). The constant of deformability (k, N/mm) was derived from the slope of this curve. For k values approaching zero, liposomes are considered deformable because they flow freely through the membrane pores. At the end of the test, the extruded sample was recovered, and the vesicle concentration was measured again by NTA to detect eventual changes in vesicle number.

In vitro skin permeability assay

In vitro skin permeability studies were performed using modified Franz diffusion cells with a diffusion area of 0.636 cm^2 and a receiver compartment of approximately 3-mL volume. Human skin was obtained from healthy volunteers undergoing abdominoplasty who signed an informed consent form. At the arrival of the skin, the excess fat was carefully removed, and full-thickness skin was cut into squares, sealed in evacuated plastic bags and stored at −20 °C until use. Epidermis sheets were obtained through mechanical separation from the remaining tissue with forceps after skin immersion in water at 60 ± 1 °C for 1 min. Prior to the experiment, the integrity of the epidermis samples was assessed by measuring the electrical impedance using a voltage of 100 mV and a frequency of 100 Hz (Agilent 4263B LCR Meter, Microlease, Italy).[26]

Human epidermis sheets were mounted on the lower half of the Franz diffusion cells with the stratum corneum facing upward. The upper and lower parts of the cell were sealed with parafilm and fastened together with a clamp. A mixture of physiological solution and ethanol (90:10 v/v) was used as the receiver medium, which was maintained under stirring and at 37±1 °C (32 ± 1 °C at the skin surface) by means of a circulating water bath. One hundred microlitres of liposome dispersion at the same RSV content was loaded in the donor chamber, and the experiment was carried out under nonocclusive conditions. A saturated RSV solution prepared using PEG/water 30/70 v/v was used as a reference. At predetermined times (1, 3, 5, 7 and 24 hours), 200 μL of receiver phase was withdrawn and replaced with fresh medium.

After 24 hours, the cells were dismounted, and epidermis sheets were recovered and washed on both sides with 5 mL methanol. After drying, the skin samples were accurately weighed and cut into small pieces prior to immersion in 5 mL of methanol for RSV extraction. Samples were bath-sonicated for 30 minutes and then incubated at 4 °C for 24 hours prior to filtration with a 0.45 μm polypropylene filter and analysed by HPLC for RSV quantification.

Statistical analysis

Comparisons among the samples were performed by analysis of variance followed by Tukey's test (OriginPro 2015, OriginLab, USA). The level of significance was taken as $p < 0.05$.

Results and Discussion

Molecular Dynamics simulations

Structural properties: Membrane Thickness and Area per Lipid

Membrane thickness was calculated as the average distance from phosphorus nuclei in the upper layer (upper P-plane) to phosphorus nuclei in the lower layer (lower P-plane) (**Figure 3B**). The P-P bilayer thicknesses averaged over the 80-ns production run are listed in **Table 2**. The values obtained are in line with the experimental values for a C18/0:2 bilayer. [27]

The projected area per lipid (APL) for each system was obtained from the xy-area of the simulation cell as $a = 2A/N$, where N = 200 is the number of lipids (**Figure 3A**). APL values averaged over the production run simulations are listed in **Table 2**.

For both quantities, the relative error is calculated as the standard deviation on 10-ns subaverages.[28]

The results show that the 2% mol/mol content of DxPE-HA is enough to lower the thickness values affecting the bending rigidity, as confirmed by the calculation of the bending modulus. APL values are comparable in the three systems.

Table 2. Production run: average values ± standard deviation for bilayer thickness, area per lipid (APL), area compressibility modulus (K_A), bending modulus (k_c) radius of gyration (R_{GYR}) of DxPE-HA molecules and end-to-end distance (D) of HA chains. The first nonsignificant digit is shown as a subscript.

System	Thickness (Å)	APL (Å^2)	K_A (N/m)	k_c (10^{-19} J)	R_{GYR} (Å)	D (Å)
SoyPC	$36.3_1 \pm 0.4_1$	$65.2_6 \pm 0.9_0$	$0.23_9 \pm 0.03_7$	$0.6_9 \pm 0.1_1$	-	-
DMPE	$34.7_0 \pm 0.3_2$	$65.2_0 \pm 0.7_0$	$0.31_1 \pm 0.05_2$	$0.7_9 \pm 0.1_4$	$32.2_6 \pm 0.4_6$	$92._3 \pm 2._4$
DOPE	$35.0_8 \pm 0.3_0$	$64.8_8 \pm 0.6_2$	$0.54_3 \pm 0.06_3$	$1.4_2 \pm 0.1_7$	$30.3_4 \pm 0.5_4$	$80._7 \pm 2._7$

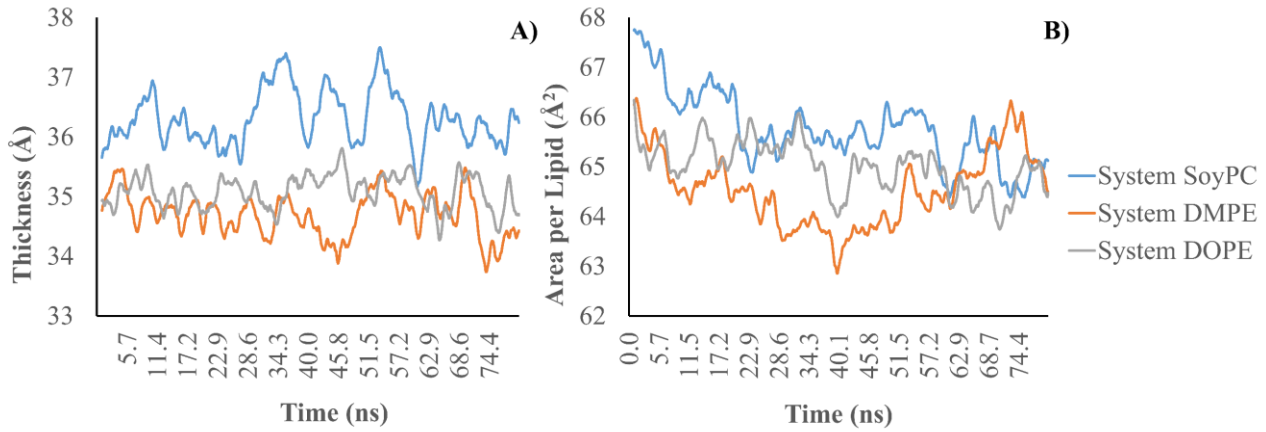

Figure 3. One-ns moving average of: A) membrane thickness, and B) area per lipid (APL) during the production run.

Area compressibility modulus and bending modulus

Average APL $\mu = \frac{1}{P}\sum_s a(s)$ – where *a(s)* is APL at time *s* and P = 80 ns – and APL variance $\sigma^2 = \frac{1}{P}\sum_s (a(s) - \mu)^2$ were used to estimate the area compressibility modulus K_A:[28]

$$K_A = \frac{2k_BT}{N}\frac{\mu}{\sigma^2} \qquad (1)$$

where k_B is Boltzmann's constant, T (K) is the absolute temperature at which the simulation is run, and $N = 200$ is the number of lipids.

Following Waheed and Edholm[28], the absolute error of APL and APL variance were estimated, respectively, by $\sigma\sqrt{\tau/T}$ and $\sigma_f\sqrt{\tau_f/T}$, where $\sigma_f = \sqrt{\frac{1}{P}\sum_s[(a(s) - \mu)^2 - \sigma^2]^2}$ and correlation time values, τ and τ_f, are defined as the integral from zero to infinity of the normalized autocorrelation functions, $g(t) = \frac{\frac{1}{P}\sum_s (a(s)-\mu)(a(s+t)-\mu)}{\sigma^2}$ and $g_f(t) = \frac{\frac{1}{P}\sum_s[(a(s)-\mu)^2-\sigma^2][(a(s+t)-\mu)^2-\sigma^2]}{\sigma_f^2}$, respectively.

A graph of the squared moduli of $g(t)$ and $g_f(t)$ for the three systems is shown in **Figure 4** with superimposed exponential curves of the general formula $e^{-2t/\tau}$. The approximate correlation times, obtained graphically, are $\tau = 1.8\ ns$ and $\tau_f = 0.8\ ns$ for System SoyPC, $\tau = 2.0\ ns$ and $\tau_f = 1.0\ ns$ for System DMPE and $\tau = 1.0\ ns$ and $\tau_f = 0.4\ ns$ for System DOPE, which correspond to a 0.2% relative error in the APL. Since the relative error was higher when calculated as the standard deviation on 10-ns subaverages, higher values were used (**Table 2)**.

APL variance values (calculated over the 80-ns production run) and absolute (relative) error (obtained from correlation times τ_f) are 1.1309 ± 0.1063 (0.0940) Å^4, 0.8678 ± 0.1042 (0.1200) Å^4 and 0.4947 ± 0.0786 (0.1005) Å^4 for System SoyPC, System DMPE and System DMPE, respectively. The relative error of K_A is then calculated for each system as the sum of the relative errors for the area and fluctuations. The corresponding values of K_A obtained from Equation (1) are listed in **Table 2**.

The value of K_A obtained for System SoyPC is in line with the experimental compressibility modulus of a C18/0:2 bilayer.[27]

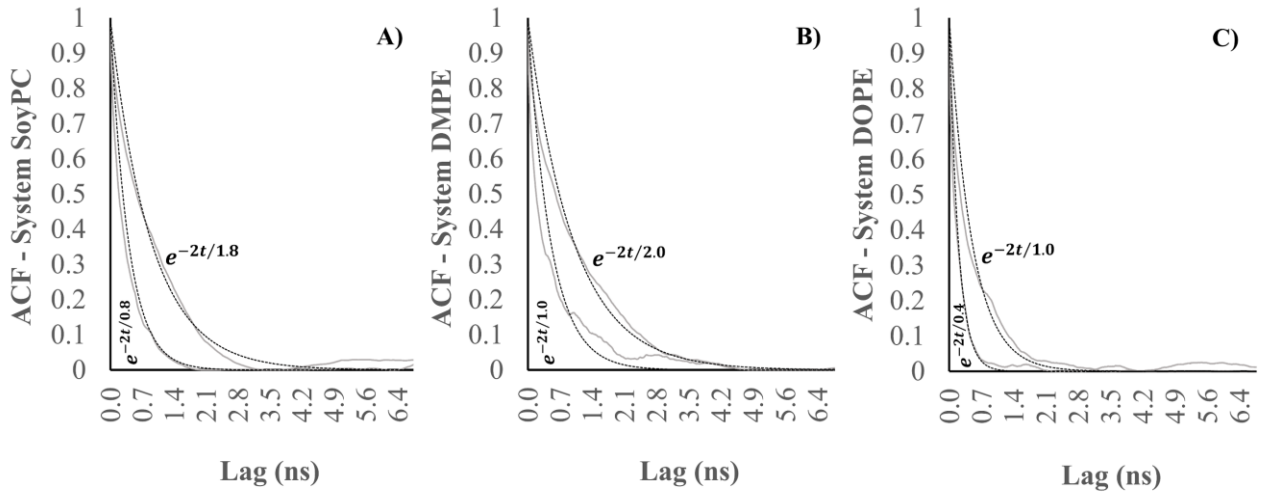

Figure 4. Squared moduli $|\mathbf{g(t)}|^2$ (upper curve, solid line) and $|\mathbf{g}_f(\mathbf{t})|^2$ (lower curve, solid line) of the normalized area autocorrelation functions (ACFs) from equations (2) and (3) for: (A) System SoyPc, (B) System DMPE and (C) System DOPE. Superimposed to the ACF are exponential curves with: (A) 1.8 ns, (B) 2.0 ns, (C) 1.0 ns decay time (higher curves, dashed lines) and (A) 0.8 ns, (B) 1.0 ns, and (C) 0.4 ns decay time (lower curves, dashed lines).

The bending modulus k_c can be estimated from K_A and the bilayer thickness, h, as[28]

$$k_c = K_A \frac{(h-h_0)^2}{24} \quad (4)$$

where and $h_0 \approx 1\ nm$. The values are listed in **Table 2**.

The calculation of the area compressibility modulus and bending modulus shows that the membrane stiffness and bending rigidity increase in the order System SoyPC < System DMPE < System DOPE. This result is in agreement with the results obtained from the experimental data.

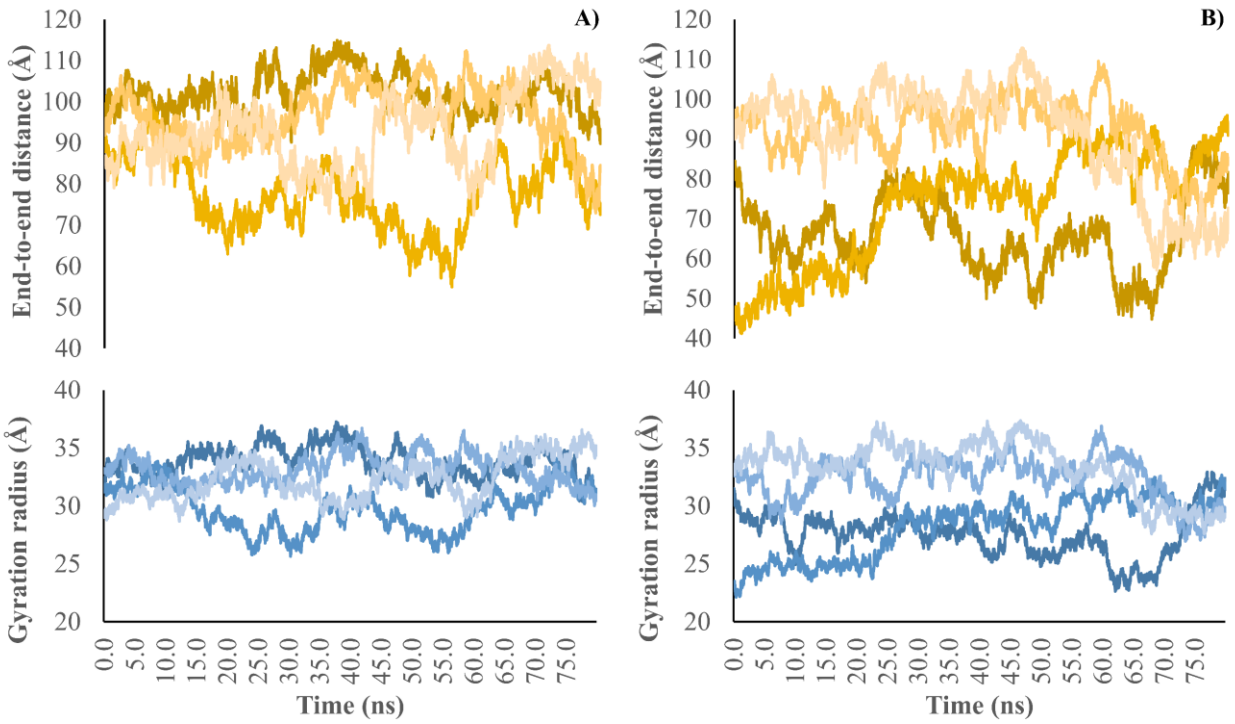

Figure 5. Dynamic profiles of end-to-end distance and radius of gyration computed from the equilibration run simulations for: A) System DMPE and B) System DOPE. The individual values obtained for each of the four DxPE-HA molecules in the simulation cell are shown in different shades.

Radius of Gyration and end-to-end distance of HA chains

To analyse the conformational profiles of the simulated HA chains, two molecular descriptors were monitored, namely, the radius of gyration (which describes molecular size and shape) and the (highly correlated) end-to-end distance of the HA chains, as an indication of chain flexibility (**Figure 5**). [16]

Values averaged over the production run simulations are listed in **Table 2.** For both quantities, the relative error is calculated as the standard deviation on 10-ns subaverages.[28] Higher values of either correspond to more extended conformations.

Analysis of the radius of gyration and the end-to-end distance suggests that HA chains in System DMPE are, on average, more extended than those same parameters in System DOPE. This result is due to a higher interchain variability in System DOPE (**Figure 5**). This effect can be ascribable either to simulation artefacts (random collisions with solvent molecules and other chains) or to the fusogenic nature of DOPE and the nonreproducibility of DOPE insertion in the bilayer, also suggested by experimental findings (Table 3)

Physicochemical features of prepared liposomes

Liposomes present a particle size ranging between 130 and 150 nm with a narrow distribution (PdI ≤ 0.1; **Table 3**). As expected, the presence of HA on the surface of liposomes causes a shift of the ζ potential towards more negative values even if any relationship with the HA loaded amount can be found. However, the contribution of HA to the ζ potential seems to be stronger in the formulations prepared by the postinsertion method, suggesting that the hydration method does not lead to a homogeneous distribution of HA on the internal and external surface of the liposomal bilayer (**Table 3**).

Table 3. Main physicochemical and mechanical features of placebo liposomes (mean ± sd of three batches).

Formulation	d (nm)	PdI	ζ (mv)	Lipids (nmol/µl)	[HA] (mg/mL)	K (N/mm)
L	146.8 ± 23.0	0.14 ± 0.10	-4.1 ± 2.0	29.8 ± 4.4	-	0.005 ± 0.003
L-DMPE PI	141.4 ± 3.0	0.06 ± 0.04	-2.99 ± 0.1	26.1 ± 2.4	-	0.007 ± 0.002
L-DMPE H	131.7 ± 0.8	0.08 ± 0.01	-2.34 ± 0.8	28.5 ± 1.5	-	0.003 ± 0.003
L-DOPE PI	146.1 ± 2.0	0.08 ± 0.03	-2.77 ± 0.2	26.2 ± 2.1	-	0.005 ± 0.003
L-DOPE H	137.8 ± 2.6	0.06 ± 0.01	-2.70 ± 0.2	29.5 ± 3.2	-	0.004 ± 0.005
L-DPPE-HA H	154.7 ± 7.9	0.11 ± 0.06	-10.9 ± 4.4	21.2 ± 1.5	1.3 ± 0.5	0.206 ± 0.028
L-DPPE-HA PI	143.2 ± 3.6	0.11 ± 0.01	-13.6 ± 1.1	18.9 ± 1.5	0.3 ± 0.1	0.175 ± 0.026
L-DMPE-HA H	127.1 ± 2.6	0.07 ± 0.02	-14.5 ± 0.2	17.5 ± 1.3	0.8 ± 0.1	0.062 ± 0.029
L-DMPE-HA PI	139.5 ± 2.1	0.07 ± 0.01	-17.8 ± 3.4	16.1 ± 0.5	0.3 ± 0.1	0.025 ± 0.003
L-DOPE-HA H	148.4 ± 8.5	0.08 ± 0.02	-26.1 ± 7.0	17.2 ± 6.4	0.7 ± 0.4	0.120 ± 0.110
L-DOPE-HA PI	142.6 ± 3.0	0.08 ± 0.02	-32.4 ± 2.1	20.0 ± 2.6	0.9 ± 0.4	0.024 ± 0.013

Within the L-HA-PI series, the highest efficiency of HA decoration was obtained using DOPE as a lipid anchor, probably due to the well-known fusogenic properties of this phospholipid, which allows easier insertion into the already formed bilayer during the postinsertion protocol. Accordingly, L-HA-DOPE-PI liposomes present the most negative values of ζ potential among all prepared liposomes.

The nature of the lipid anchor seems instead to have no influence on RSV encapsulation, regardless of the preparation method. The encapsulation efficacy was not significantly different for all RSV-loaded liposomes and in all cases was approximately 60% (**Table 4**).

Deformability

In a previous study, we demonstrated that the addition of PE with a quite high T_m, such as DPPE, leads to a significant increase in the stiffness of the bilayer, requiring the addition of a further fluidizing agent in the composition of liposomes[10]. Decreasing the DPPE concentration to 1.5%

mol/mol using the postinsertion approach did not change this behaviour (**Table 3**), since the K value was found to be out of the limit admitted for (trans)dermal administration.[25] Collectively, the number of vesicles/mL measured by NTA at the end of the deformability test almost halved, moving from $115.0 \times 10^9 \pm 13.4 \times 10^9$ to $71.2 \times 10^9 \pm 12.6 \times 10^9$. The reduction in the number of particles was due to the formation of aggregates or larger vesicles with a size in the 250-300 nm range.

Table 4 Main physicochemical and mechanical features of RSV liposomes (mean ± sd of three batches).

		L-DMPE-HA H	L-DMPE-HA PI	L-DOPE-HA PI
D	(nm)	135.7 ± 0.7	134.0 ± 0.8	135.6 ± 0.2
PdI		0.06 ± 0.01	0.04 ± 0.01	0.05 ± 0.01
ζ	(mv)	-16.2 ± 3.1	-12.7 ± 0.3	-22.3 ± 3.3
Lipids	(nmol/µl)	18.8 ± 1.2	18.6 ± 2.0	19.4 ± 0.3
[HA]	(mg/mL)	1.1 ± 0.1	0.5 ± 0.1	1.1 ± 0.3
EE	(%)	65.00±6.83	59.10 ± 4.39	60.85± 3.80
K	(N/mm)	0.053 ± 0.012	0.037 ± 0.012	0.043 ± 0.010

In contrast, neither DMPE nor DOPE affected the intrinsic rigidity of the bilayer since k values were on the same order of magnitude as those values of plain liposomes (**Table 3**). The most prominent effect on liposome deformability seemed then to rely on the presence of the polysaccharide in the formulation since all HA-decorated liposomes presented a K value at least 10-fold higher than similar formulations without HA. The effect seemed to be dose-dependent since the formulations prepared by postinsertion showed lower K than liposomes prepared by the film hydration method. We may also hypothesize that this behaviour depends on the distribution of the polysaccharide within the bilayer and that the presence of HA on the internal face of the bilayer exerts an important stiffening effect on the membrane, also considering that the deformability is measured by a test carried out in compression mode. The replacement of DPPE with DMPE, a PE with a shorter acyl chain and slightly lower T_m, as an anchor of HA allowed us to maintain the flexibility of the bilayer in the acceptance range regardless of the preparation method and, thus, lipid concentration (**Table 3**). In contrast, the insertion of the DOPE conjugate at the highest concentration (L-DOPE-HA-H) altered the rearrangement properties of the membrane. In line with predicted K_A and k_c values derived from MD simulations (**Table 2**), L-DOPE-HA-H shows a higher k value, along with a higher variability of the experimental data. Consistently, L-DOPE-HA-H was the only formulation that experienced a very important loss of intact vesicles after extrusion, as depicted in **Figure 6A**. Since the conformational profile and geometry of HA in the DMPE-HA and DOPE-HA systems were found to be comparable,

the different behaviour should be ascribed to the lipid anchor itself. These data were unexpected, considering the low T_m of the lipid (lower than 0 °C). Nevertheless, owing to the fusogenic nature and the nonlamellar structure of DOPE, lipids might insert into the bilayer in a nonreproducible manner, as also suggested by the results from MD simulations. Based on deformability properties resulting from the combined experimental and in silico approach, the formulation containing the DOPE-HA conjugate produced by the hydration method was discarded from the set of formulations selected for the in vitro skin permeability assay, and then the RSV-loaded formulation was not prepared. In all other cases, RSV-containing formulations were tested for their mechanical properties to rule out that the insertion of the drug into the bilayer could change the behaviour of the vesicles under stress, and RSV was found not to affect the deformability properties of the formulations under test that were then all used for the in vitro skin permeability assays (**Table 4**).

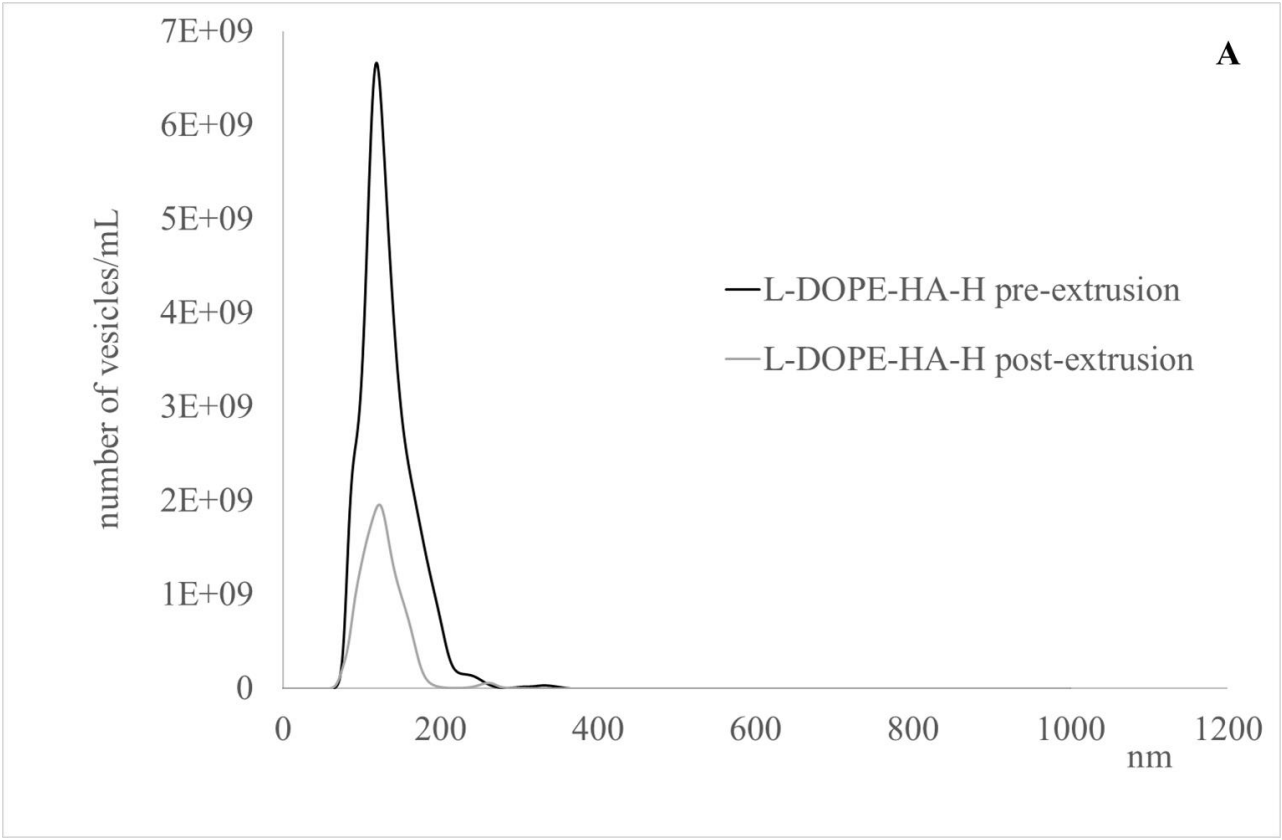

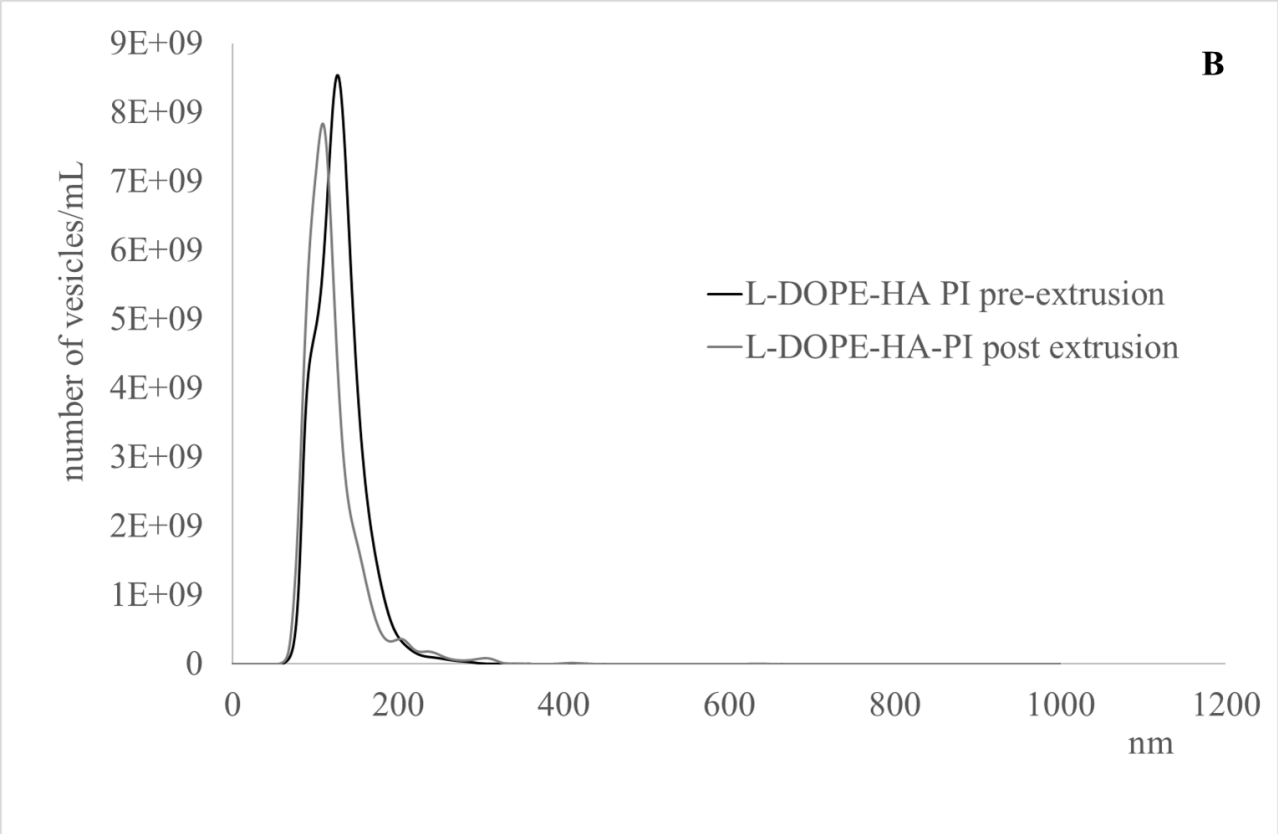

Figure 6- Representative particle size distribution of L-DOPE-HA-H (A) and L-DOPE-HA-PI (B) liposomes before and after the deformability assay obtained by nanoparticle tracking analysis (NTA). The data are the mean of five measurements and clearly show the significant decrease in vesicle count after passage of L-DOPE-HA-H liposomes through the 50-nm pores.

In vitro skin permeability

RSV is well known to exhibit very poor passive diffusion through the skin, and its deposition in the tissue is even worse. In contrast to the control RSV solution in which the permeated amount was not quantifiable, the encapsulation of RSV in plain liposomes allowed at least the detection of the drug both in receptor fluid and in the epidermis, but the penetration pattern was very weak (**Figure 7**). The decoration of the liposomal surface with HA moieties led to an increase in the permeated amount of the drug through the skin in all cases. However, permeation of RSV carried by HA-decorated liposomes was significantly higher than the permeation of RSV carried by control liposomes only for the DMPE-HA-PI formulation (**Figure 7**), with an increase in the permeated amount after the 24-h experiment (Q_{24}) of at least 5 times ($p<0.05$). In the first instance, a low HA content on the surface of liposomes seems to then favour RSV permeation, which might be ascribed to an increased partitioning of the RSV-liposomes in the epidermis as a result of the well-known hydration effect of HA[9] and its ability to cause an impairment of the skin barrier by forming hydrophobic complexes with SC phospholipids[29]. Both of these mechanisms contribute to creating preferential paths for

vesicle penetration. Above a certain concentration of polysaccharide on the surface, retention in the epidermis seems to be favoured rather than permeation due to the high affinity of HA for skin keratins **Errore. Il segnalibro non è definito.** (**Table 5**). This trend was highlighted by calculating R_{24}/Q_{24}, which can be considered a descriptor of the affinity of a species for the epidermis layers[26]. Accordingly, L-DOPE-HA PI RSV exposed the highest HA amount on the outer surface of the liposome membrane and showed the lowest R_{24}/Q_{24} ratio.

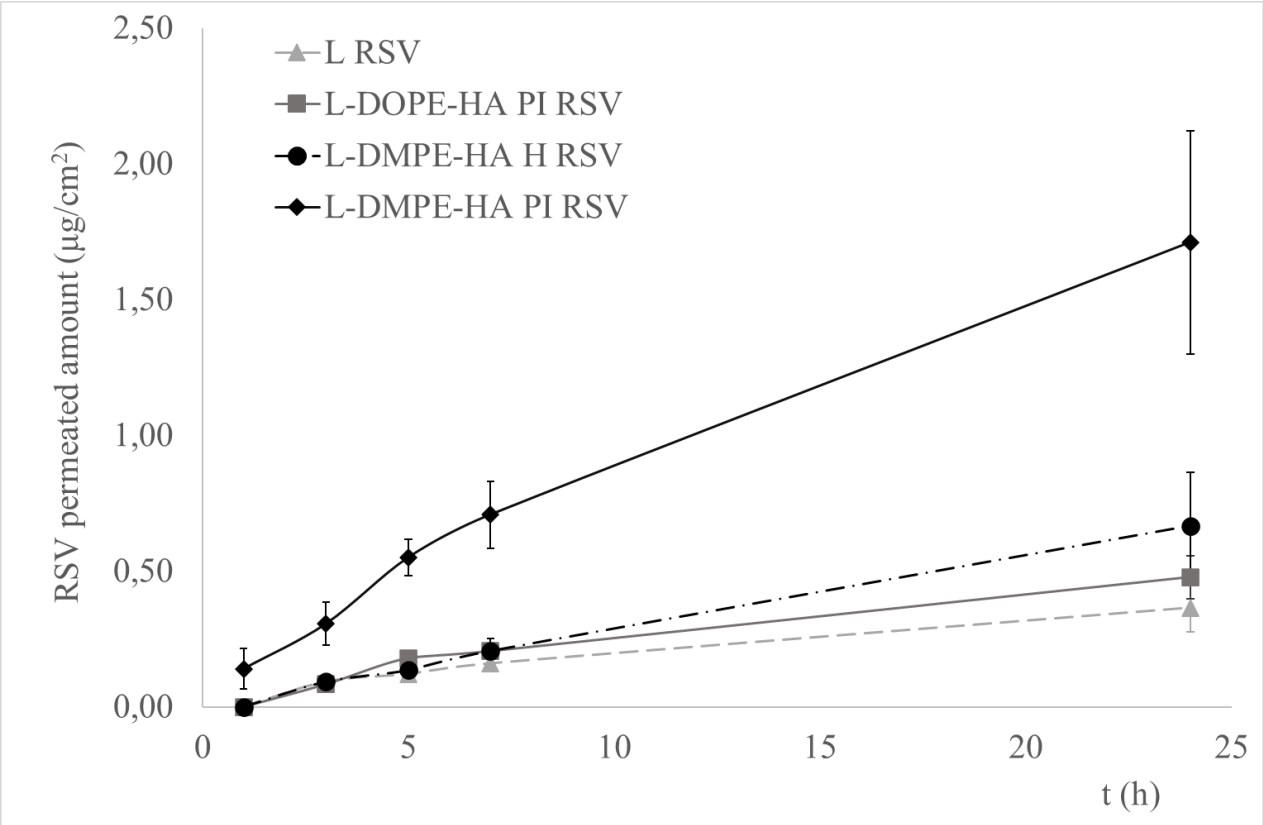

Figure 7- In vitro skin permeation profile of RSV encapsulated in plain and HA-decorated liposomes through human epidermis. Only formulations with suitable deformability properties were tested.

Since any significant difference in both deformability properties (k value and K_A) and HA conformation (radius of gyration and end-to-end distance) was detected for DOPE-HA-PI and DMPE-HA-PI liposomes, the different penetration patterns of the tested liposomes seemed to be ascribable only to the HA superficial concentration. To confirm the dose dependence of HA-decorated liposomes, two further liposomal formulations having the same lipids (DMPE and DOPE) but a lower HA content were obtained by using 0.3% mol/mol of DOPE-HA and DMPE-HA conjugates by the postinsertion method. As depicted in **Figure 8**, the permeation of RSV increases the HA content (expressed as HA/phospholipid weight/mol ratio) up to a threshold concentration, above which the trend is completely inverted in favour of the accumulation of the model drug in the skin, demonstrating the key role exerted by HA as a localizing agent.

Table 5- Permeated (Q) and accumulated (R) amounts of RSV in the skin after the 24-h experiment and R_{24}/Q_{24} values calculated for the main liposomal formulations in the study

	R_{24}/Q_{24}	Q24	R24 (μg/mg)
L RSV	0.67	0.36± 0.18	0.24 ± 0.08
L-DOPE-HA PI RSV	1.33	0.48± 0.20	0.64 ± 0.02
L-DMPE-HA H RSV	0.88	0.66 ± 0.34	0.58 ± 0.13
L-DMPE-HA PI RSV	0.21	1.71 ± 0.71	0.36 ± 0.20

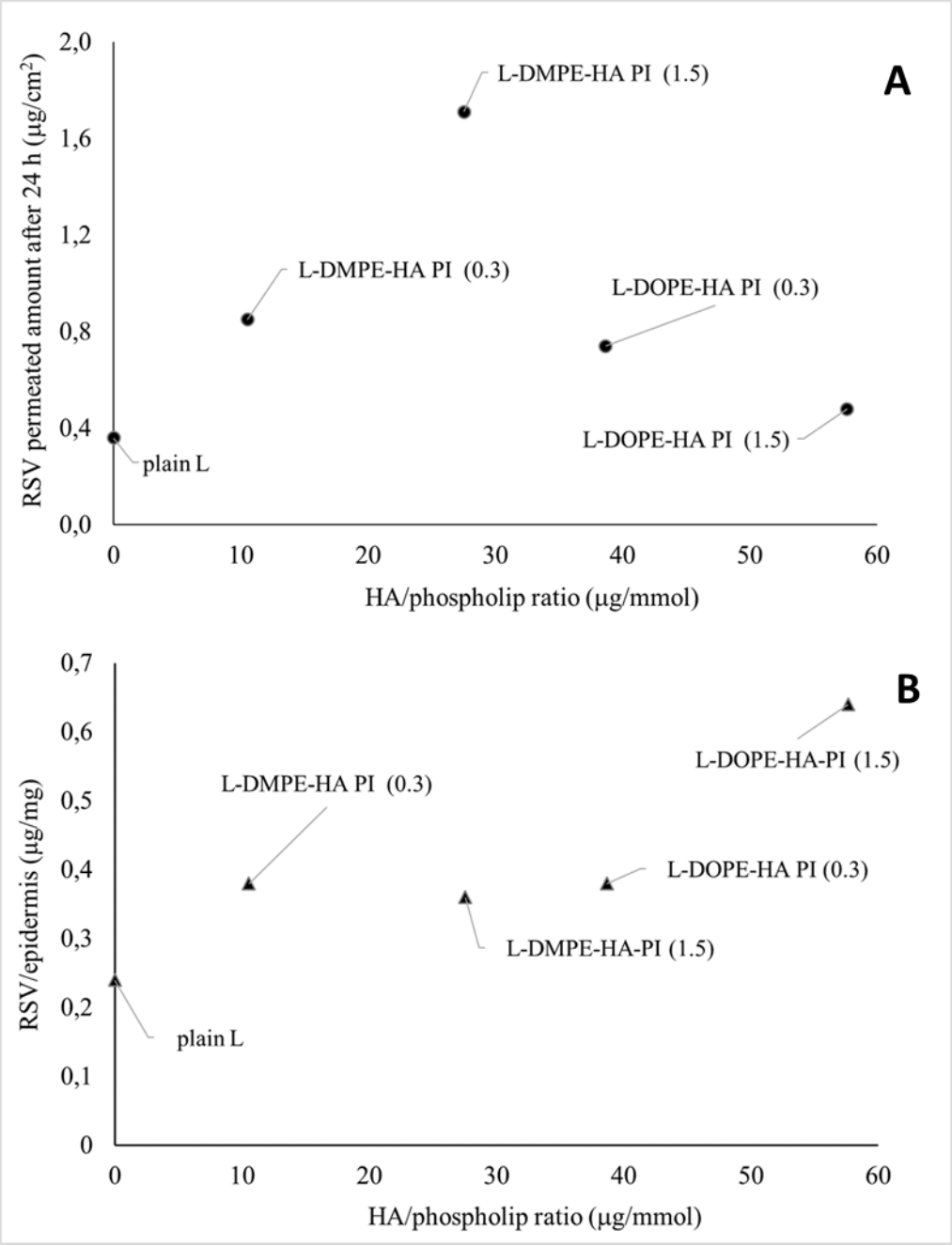

Figure 8- Trend of RSV permeation (A) and deposition (B) in the skin as a function of hyaluronan content on the membrane of liposomes. Each point represents the mean of three different experiments.

Conclusions

The experimental data demonstrated that phosphoethanolamine chemistry affects both the deformability of liposomes (with DMPE being the best choice) and the amount of HA inserted within liposome membrane. Along with phospholipid anchor and HA amount, liposome deformability is also affected by the localization of the polysaccharide on liposome membrane, resulting higher for liposomes having HA exposed only on the outer face of the membrane. These features determined the skin penetration pattern of RSV. To the best of our knowledge, this is the first evidence of the feasibility of tuning the retention of a drug in the epidermis by modulating the targeting moiety dose and disposition. In other words, deformable HA-liposomes can be exploited to modulate the fate of a drug applied on the skin, favouring the localization of the carried drug in the epidermis for the treatment of local diseases or its permeation for the treatment of deeper diseases, depending on the physicochemical features of the carried drug. Finally, the MD simulations, performed on a specific model membrane composed of Soy PC, a DxPE anchor and a HA chain, showed a good relationship among the structural properties of lipid bilayers, including elastic properties such as the area compressibility modulus and the bending modulus and the experimental deformation properties. These results confirm that MD simulations predicting the bilayer rigidity of liposomal formulation, can be a useful tool in designing decorated liposomes independently of the administration route or therapeutic target.

Bibliography

[1] How, K.N.; Yap, W.H.; Lim, C.L.H.; Goh, B.H.; Lai, Z.W. Hyaluronic Acid-Mediated Drug Delivery System Targeting for Inflammatory Skin Diseases: A Mini Review. *Front Pharmacol.* **2020,** 11, 1-8.

[2] Honeywell-Nguyen, P-L; Bouwstra, J.A. Vesicles as a tool for transdermal and dermal delivery. *Drug Discov Today Technol* **2005**, 2(1), 67-74.

[3] Morilla, M.J.; Romero, E.L. Carrier deformability in Drug Delivery. *Curr. Pharm. Des*. **2016**, 22, 1118 – 1134.

[4] Natsheh, H.; Touitou, E. Phospholipid Vesicles for Dermal/Transdermal and Nasal Administration of Active Molecules: The Effect of Surfactants and Alcohols on the Fluidity of Their Lipid Bilayers and Penetration Enhancement Properties. *Molecules* **2020**, *25*, 1-42.

[5] Zhu, J.; Tang, X.; Jia, Y.; Ho, C.; Huang, Q. Applications and delivery mechanisms of hyaluronic acid used for topical/transdermal delivery – A review. *Int J Pharm* **2020**, 578, 119127, 1-10.

[6] Muto, J.; Sayama, K.; Gallo, R.L.; Kimata, K. Emerging evidence for the essential role of hyaluronan in cutaneous biology. *J Dermatol Sci.* **2019**, 94(1), 190-195.

[7] Brown, M.B.; Jones, S.A. Hyaluronic acid: a unique topical vehicle for the localized delivery of drugs to the skin. *J Eur Acad Dermatol Venereol.* **2005,** 19(3), 308-318.

[8] Brown, M.B; Hanpanitcharoen, M.; Martin, G.P. An in vitro investigation into the effect of glycosaminoglycans on the skin partitioning and deposition of NSAIDs. *Int J Pharm.* **2001,** 225(1-2), 113-121.

[9] Witting, M.; Boreham, A.; Brodwolf, R.; Vávrová, K.; Alexiev, U.; Friess, W.; Hedtrich, S. Interactions of hyaluronic acid with the skin and implications for the dermal delivery of biomacromolecules. *Mol. Pharm.* **2015**, 12, 1391-1401.

[10] Franzé, S.; Marengo, A.; Stella, B.; Minghetti, P.; Arpicco, S.; Cilurzo, F.Hyaluronan-decorated liposomes as drug delivery systems for cutaneous administration. *Int J Pharm* **2018**, 535 (1-2), 333-339.

[11] Cheng, C-Y.; Lin, Y-K.; Yang, S-C.; Alalaiwe, A.; Lin, C-J.; Fang, J-Y.; Lin, C-F. Percutaneous absorption of resveratrol and its oligomers to relieve psoriasiform lesions: In silico, in vitro and in vivo evaluations. *Int J Pharm* **2020**, 585, 1-14.

[12] Scognamiglio, I.; De Stefano, D.; Campani, V.; Mayol, L.; Carnuccio, R.; Fabbrocini, G.; Ayala, F.; La Rotonda, M.I.; De Rosa, G. Nanocarriers for topical administration of resveratrol: A comparative study, *Int J Pharm* **2013**, 440 (2), 179-187.

[13] Nastiti, C.M.R.R.; Ponto, T.; Mohammed, Y.; Roberts, M.S.; Benson, H.A.E. Novel Nanocarriers for Targeted Topical Skin Delivery of the Antioxidant Resveratrol. *Pharmaceutics* **2020**, 12(2), 1-15.

[14] Arpicco, S.; Lerda, C.; Dalla Pozza, E.; Costanzo, C.; Tsapis, N.; Stella, B.; Donadelli, M.; Dando, I.; Fattal, E.; Cattel, L.; Palmieri, M. Hyaluronic acid-coated liposomes for active targeting of gemcitabine. *Eur J Pharm Biopharm*. **2013**, 85(3), 373-80.

[15] Pedretti, A.; Villa, L.; Vistoli, G. VEGA: A Versatile Program to Convert, Handle and Visualize Molecular Structure on Windows-Based PCs. *J. Mol. Graph. Model*. **2002** https://doi.org/10.1016/S1093-3263(02)00123-7.

[16] Cilurzo, F.; Vistoli, G.; Gennari, C.G.; Selmin, F.; Gardoni, F.; Franzè, S.; Campisi, M.; Minghetti, P. The role of the conformational profile of polysaccharides on skin penetration: the case of hyaluronan and its sulfates. *Chem Biodivers*. **2014**, 11(4), 551-561.

[17] Tarini, M.; Cignoni, P.; Montani, C. Ambient Occlusion and Edge Cueing for Enhancing Real Time Molecular Visualization. *IEEE Transactions on Visualization and Computer Graphics* **2006**, 12 (5) , 1237-1244.

[18] Phillips, J.C.;, Hardy, D.J.; Maia, J.D.C.; Stone, J.E.; Ribeiro, J.V.; Bernardi, R.C.; Buch, R.; Fiorin, G.; Hénin, G.; Jiang, W.; McGreevy, R.; Melo, M.C.R.; Radak, B.K.; Skeel, R.D.; Singharoy, A.; Wang, Y.; Roux, B.; Aksimentiev, A.; Luthey-Schulten, Z.; Kalè, L.V.; Schulten, K.; Chipot, C.; Tajkhorshld, E. Scalable molecular dynamics on CPU and GPU architectures with NAMD. *J. Chem. Phys*. **2020,** 153; https://doi.org/10.1063/5.0014475

[19] Klauda, J.B.; Venable, R.M.; Freites, J.A.; O'Connor, J.W.; Tobias, D.; Mondragon-Ramirez, C.; Vorobyov, I.; MacKerell, A.; Pastor, R.W. Update of the CHARMM all-atom additive force field for lipids: validation on six lipid types. *J. Phys. Chem. B* **2010,** 114, 7830-7843.

[20] Jorgensen W.L.; Chandrasekhar, J.; Madura, J.D. Comparison of simple potential functions for simulating liquid water. *Journal of Chemical Physics.* **1983,** 79(2), 926–935.

[21] Aho, A.V.; Kernighan, B.W.; Weinberger, P.J. The Awk Programming Language. *Addison Wesley Publiching Company*, **1987**. ISBN-13 : 978-0201079814

[22] Rocco, P.; Cilurzo, F.; Minghetti, P.; Vistoli, G.; Pedretti, A. Molecular Dynamics as a tool for in silico screening of skin permeability. *Eur J Pharm Sci.* **2017**, 106, 328-335.

[23] Rouser, G.; Fleischer, S.; Yamamoto, A. Two dimensional thin layer chromatographic separation of polar lipids and determination of phospholipids by phosphorus analysis of spots. *Lipids* **1970**, 5, 494-496.

[24] Bitter, C.T.H.; Muir, M. A modified uronic acid carbazole reaction. *Anal. Biochem*. **1962**, 4, 330-334.

[25] Franzè, S.; Donadoni, G.; Podestà, A.; Procacci, P.; Orioli, M.; Carini, M.; Minghetti, P.; Cilurzo, F. Tuning the extent and the depth of penetration of flexible liposomes in human skin. *Mol. Pharm.* **2017**, 14, 1998-2009.

[26] Franzè, S.; Gennari, C.G.M.; Minghetti, P.; Cilurzo, F. Influence of chemical and structural features of low molecular weight heparins (LMWHs) on skin penetration. *Int J Pharm* **2015**, 481(1–2), 79-83.

[27] Rawicz, W.; Olbrich, K.C.; McIntosh, T.; Needham, D.; Evans, E. Effect of chain length and unsaturation on elasticity of lipid bilayers. *Biophys J*. **2000**, 79(1), 328-339.

[28] Waheed, Q.; Edholm, O. Undulation contributions to the area compressibility in lipid bilayer simulations. *Biophys J*. **2009,** 18, 97(10), 2754-2760.

[29] Jung, H.; Kim, K.; Yun, S.; Hahn, S. Enhancing the transdermal penetration of nanoconstructs: could hyaluronic acid be the key? *Nanomedicine* **2014**, 9(6), 743–745.